Bull Volcanol (2006) 68: 363–376
DOI 10.1007/s00445-005-0017-6

RESEARCH ARTICLE

K. Mee · H. Tuffen · J. S. Gilbert

Snow-contact volcanic facies and their use in determining past eruptive environments at Nevados de Chillán volcano, Chile

Received: 2 March 2004 / Accepted: 19 June 2005 / Published online: 9 December 2005

Abstract Studies of the eruptive products from volcanoes with variable ice and snow cover and a long history of activity enable reconstruction of erupted palaeoenvironments, as well as highlighting the hazards associated with meltwater production, such as jökulhlaups and magma-water interaction. Existing difficulties include estimation of ice/snow thicknesses and discrimination between ice- and snow-contact lithofacies. We present field evidence from the Cerro Blanco subcomplex of Nevados de Chillán stratovolcano, central Chile, which has erupted numerous times in glacial and non-glacial periods and most recently produced andesitic lava flows in the 1861–1865 eruption from the Santa Gertrudis cone on the northwest flank of the volcano. The main period of lava effusion occurred during the winter of 1861 when the upper flanks of the volcano were reportedly covered in snow and ice. The bases and margins of the first lava flows produced are cut by arcuate fractures, which are interpreted as snow-contact features formed when steam generated from the melting of snow entered tensional fractures at the flow base. In contrast, the interiors and upper parts of these flows, as well as the overlying flow units, have autobrecciated and blocky textures typical of subaerial conditions, due to insulation by the underlying lava. Similar textures found in a lava flow dated at 90.0±0.6 ka that was emplaced on the northwest flank of Cerro Blanco, are also inferred to be ice and snow-contact features. These textures have been used to infer that a small valley glacier, overlain by snow, existed in the Santa Gertrudis Valley at the time of the eruption. Such reconstructions are important for determining the long-term evolution of the volcano as well as assessing future hazards at seasonally snow-covered volcanoes.

Keywords Nevados de Chillán · Snow-contact · Palaeoenvironment reconstruction · Hackly jointing · Columnar jointing · Pseudopillow fractures · Santa Gertrudis lava

Editorial responsibility: J. Donnelly-Nolan

K. Mee (✉) · H. Tuffen · J. S. Gilbert
Department of Environmental Science, Lancaster University, LA1 4YQ, UK
e-mail: k.mee@lancaster.ac.uk

Introduction

Interaction between magma and snow or ice can occur in a wide variety of eruptive settings, from volcanic ejecta coming into contact with small volumes of snow or ice, to eruptions under several hundred metres of ice (Smellie 2000). Eruptions under 'thick ice' (>150 m) such as the 1996 Gjálp eruption beneath Vatnajökull, Iceland (Gudmundsson et al. 1997) can produce catastrophic floods (jökulhlaups) capable of devastating infrastructure. Lahars produced by volcanic material mixing with snow and ice melt are a common hazard at glacier-covered stratovolcanoes (Gardner et al. 1994; Barberi et al. 1995; Thouret et al. 1995).

We use the term 'subglacial eruption' for any eruption that occurs entirely beneath ice, although the erupted material may eventually breach the ice surface (e.g. Smellie 2001; Tuffen et al. 2001). We use the term 'ice-constrained' for situations in which eruption products are interpreted to have been confined by ice or snow causing their forward advancement to be restricted (e.g. Lescinsky and Sisson 1998; Vinogradov and Murav'ev 1988). The term 'ice- or snow-contact' describes situations where volcanic products have come into contact with snow or ice but were not confined by it (Major and Newhall 1989; Walder 2000).

Lithofacies associations that are used to reconstruct palaeo-ice thicknesses include the subglacial hyaloclastite to subaerial lava transitions in tuyas (Jones 1970; Skilling 1994; Werner et al. 1996; Smellie 2000; Edwards et al. 2002; Tuffen et al. 2002a), and discrimination between basaltic hyaloclastite and pillow successions, emplaced beneath 'thin ice' (<150 m) and 'thick ice' (>150 m) respectively, on the basis of sedimentological evidence for contrasting meltwater drainage patterns (Smellie and Skilling 1994; Smellie 2000, 2002). The former method is relatively inaccurate, as the elevation of the passage zone, which is thought to indicate water level in an ice-dammed lake

Table 1 Summary of age data used during this study

Lithologic unit and sample no	Rock type (SiO_2 wt.%)	$^{40}Ar/^{39}Ar$ ages (analyses conducted on whole-rock cores)	Data source
Nev1b Dacite lavas (C4)	Dacite (68%)	68.1±1.0 ka	Dixon et al. 1999
Upper Santa Gertrudis Valley lavas (CB55)	Andesite (58%)	90.0±0.6 ka	This study (unpublished data from Mee 2004)
LP Los Pincheira lavas	Andesite (61%)	640±20 ka	Dixon et al. 1999

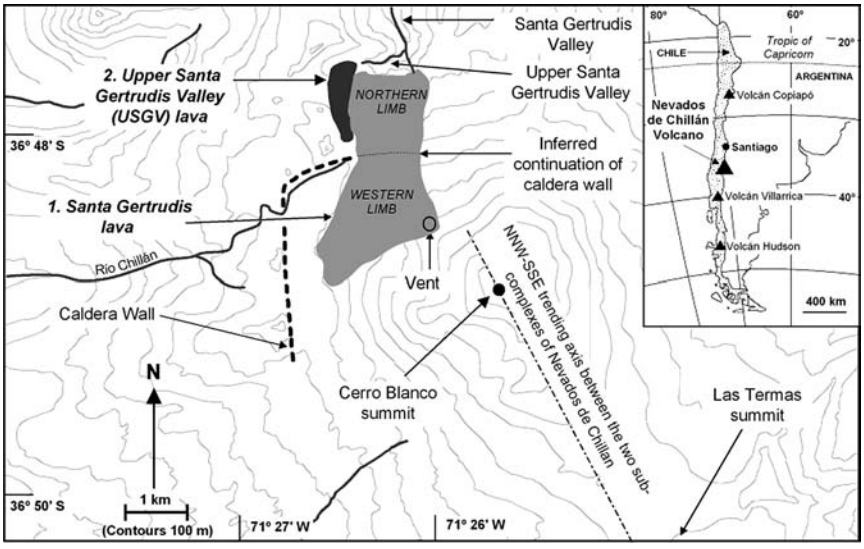

Fig. 1 Topographic map of the Cerro Blanco subcomplex of Nevados de Chillán volcano. *Inset map* shows the location of Nevados de Chillán and some other major volcanoes within Chile

during an eruption, may be as much as 100–150 m beneath the palaeo-ice surface (Smellie 2000), possibly due, in part, to the formation of a deep cauldron in the ice surface (Gudmundsson et al. 1997). The second method can only provide information on relative ice thicknesses rather than absolute values. The relationship between the volatile content of subglacially erupted glasses to the overlying ice thickness, which has also been employed as a thickness indicator (Moore and Calk 1991; Moore et al. 1995; Dixon et al. 1999), is ambiguous, because the pressure in subglacial cavities where magma is quenched may be considerably lower than glaciostatic pressure (Tuffen et al. 2002b).

Identification of lava flows that have interacted with ice has provided information on the extent of ice cover (e.g. Gilbert et al. 1998; Lescinsky and Sisson 1998; Lescinsky and Fink 2000; Wilch and McIntosh 2000; Helgason and Duncan 2001; Edwards et al. 2002) at the time of eruption, with implications for eruptive hazards and the timing of glacial advances and retreats associated with global or regional climate change. However, accurate reconstruction of the ice thickness is usually impossible unless additional information, such as the maximum elevation of glacial erosion (Mathews 1951), is available.

At Nevados de Chillán volcano (Fig. 1), central Chile, a pilot study has been carried out to test the combined use of ice-constrained, subaerial and newly-identified snow-contact facies as tools for more accurately reconstructing palaeo-ice thicknesses. Field observations and $^{40}Ar/^{39}Ar$ dating of key volcanic units have allowed detailed reconstruction of former eruptive environments at Nevados de Chillán, and have provided new insight into interaction between magma and snow/ice at stratovolcanoes. Table 1 summarises the age data used for this study.

Geologic setting

Nevados de Chillán is a large stratovolcano of intermediate composition consisting of two compositionally distinct volcanic centres (Dixon et al. 1999) situated ~6 km apart on a NNW-SSE-trending axis (Figs. 1 and 2). It is situated ~400 km south of Santiago, Chile, in the Southern Volcanic Zone (SVC) of the Andean Cordillera (Dixon et al. 1999). The Cerro Blanco subcomplex to the northwest is dominantly andesitic and the southeastern Las Termas subcomplex is predominantly dacitic (Dixon et al. 1999). Nevados de Chillán has been active since at least 640±20 ka (Dixon et al. 1999). The most recent activity from the Cerro Blanco subcomplex took place between 1861 and 1865 and formed the Santa Gertrudis lava field (Dixon et al. 1999). Eruptions at the Las Termas subcomplex occurred as recently as 1906–1948 1973–1986 (Dixon et al. 1999) and 2003 (Global Volcanism Program). Nevados de Chillán has been active during numerous Quaternary glacial and interglacial periods, producing complex associations of subaerial and subglacial lavas, pyroclastic flow deposits, ash fall deposits, lahar deposits and scoria cones (Dixon et al. 1999).

The most extensive of the ice-constrained facies are the ~200 m thick, columnar jointed Los Pincheira lavas

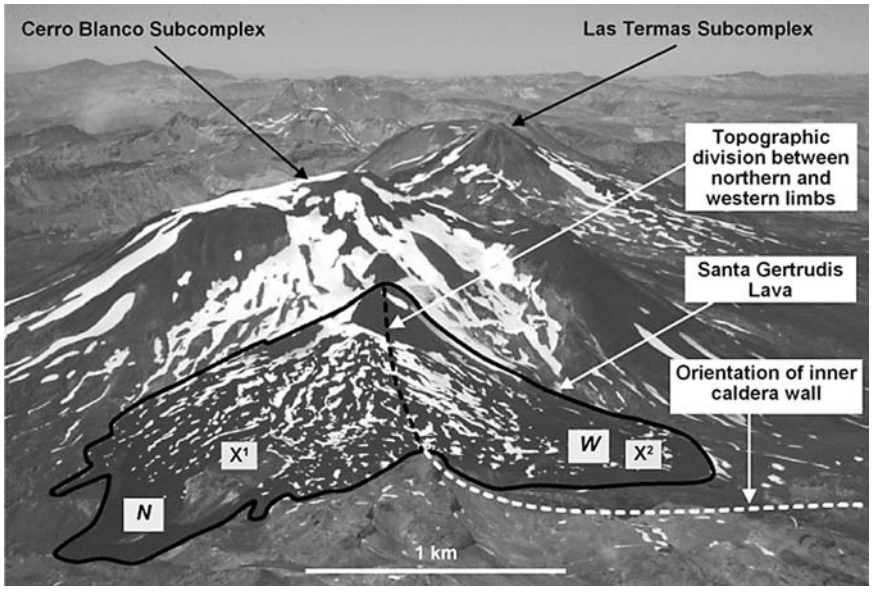

Fig. 2 The Santa Gertrudis lava (*outlined*) on the northwest flank of Nevados de Chillán volcano, viewed looking to the east with the Las Termas subcomplex in the background. χ^1 and χ^2 refer to the locations of Figs. 6 and 7, respectively; *N* and *W* refer to the northern and western limbs of the Santa Gertrudis lava

(Fig. 3a). These andesitic lavas were erupted into the glaciated valleys surrounding the volcano at 640±20 ka (Dixon et al. 1999), have an estimated uneroded volume of 10 km^3 and can be traced up to 35 km away from the volcano. The great thickness of the flows is thought to be due to confinement as the forward progress of the lava was impeded by the need to melt glacial ice (e.g. Lescinsky and Sisson 1998). The Nev1b Dacite (Table 1) is columnar jointed lava that was emplaced at 68.1±1.0 ka (Dixon et al. 1999) in an eruption during the Marine Oxygen Isotope Stage (MOIS) 4 glacial period. Subglacial facies at Nevados de Chillán, of unknown age, include glassy, hackly jointed lava bodies associated with poorly sorted, massive hyaloclastite (Fig. 3b).

The Santa Gertrudis eruption

The andesitic Santa Gertrudis lava was erupted between 1861 and 1865 on the northwestern flank of the Cerro Blanco subcomplex (Fig. 2). Although there was no great volume of ice on Nevados de Chillán between 1861 and 1865, the main phase of the eruption occurred during August of 1861 (southern hemisphere winter) when seasonal snow covered the upper flanks of the volcano (Petit-Breuilh 1995). Features around the margins of the lava, in conjunction with eyewitness reports from the time of the eruption, suggest that the lava was erupted subaerially but flowed over seasonal snow. Eyewitness reports and scientific papers from the time of the eruption have been compiled by Petit-Breuilh (1995). The chronology of events and a list of observations for the eruption of the Santa Gertrudis lava are summarised in Table 2.

Santa Gertrudis lava

The northern and western flanks of Cerro Blanco are cut by inward-facing, arcuate cliffs (Fig. 4) interpreted as remnants of a caldera wall (Déreulle and Déreulle 1974). At the northern end, the wall curves inward toward the summit of Cerro Blanco, effectively producing a barrier between the western and northern flanks of Cerro Blanco (Fig. 2). When the Santa Gertrudis lava was erupted between 1861 and 1865, it flowed on both sides of the northern end of the caldera wall. As a result, the Santa Gertrudis lava has two discrete limbs (Figs. 2 and 5): the first stretching north over the top and beyond the caldera wall towards the top of the Santa Gertrudis Valley (Fig. 1), the second stretching west onto a flat-lying area inside the caldera wall (Fig. 4). The caldera wall cliffs are composed of andesite lavas, which dip gently to the west away from the volcano and are dissected by drainage outlets feeding the Chillán River to the west (Fig. 1). The true thickness of the Santa Gertrudis lava is unknown since cross-sections through the lava field are absent; however, through field observations, we estimate it to be between 5 m (at the margins of the lava) and 20 m (in the central regions of the lava). It has an estimated preserved volume of ca. 2 km^3 (from combined use of field observations and aerial photographs), and can be separated into two main textural facies: the crystalline flow interior and the glassy flow margin (Fig. 5).

Lava flow interior

The flow interior facies dominates the exposed surface of the Santa Gertrudis lava. It mostly crops out in the upper parts of the lava field on the flanks of the Santa Gertrudis cone, and is separated from the flow margin on the western limb by a flattish zone composed of tephra and scree. The flow interior consists of blocky, vesicular, porphyritic and non-glassy andesite lava (Fig. 6) with scoriaceous autobreccia and oxidised surfaces. On fresh faces the lava is dark grey, holocrystalline and vesicular.

At the edge of the flow interior facies, a gradational contact over several metres gives way to a mixed zone 5–10 m

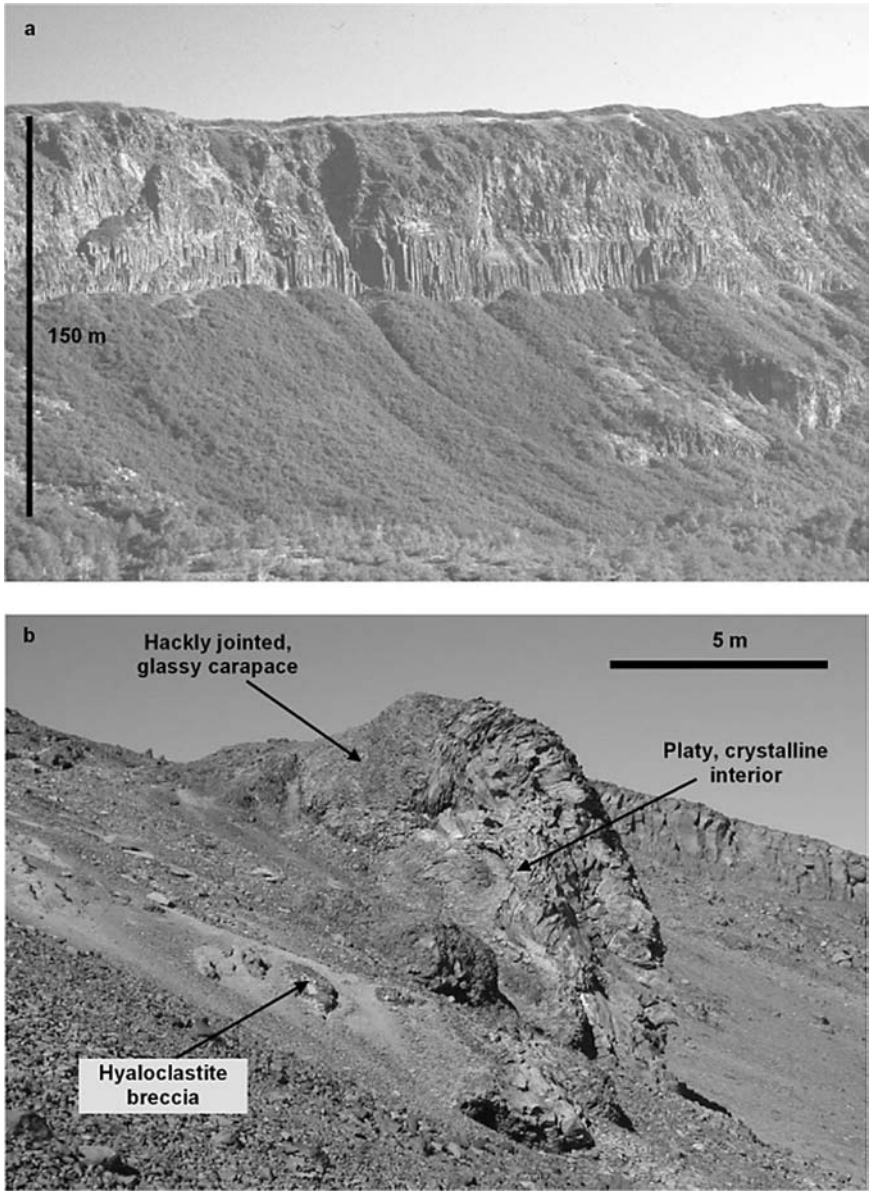

Fig. 3 Two examples of subglacial or ice-constrained facies at Nevados de Chillán volcano: **a** the columnar jointed Los Pincheira lavas were erupted into the glaciated valleys surrounding the volcano at 640 ka, and are up to 200 m in height; **b** a subglacial lava lobe with a hackly jointed and quenched outer carapace and surrounded by hyaloclastite

Table 2 Chronology for the 1861–1865 eruption from the Santa Gertrudis cone, NW Cerro Blanco (based on Petit-Breuilh 1995)

Date	Observations
June 1861	Eruption commences from Santa Gertrudis cone on northwest flank of Cerro Blanco. Small smoke column was evident. Ejected bombs seen at night from Chillán (80 km west)
August 2nd 1861	Explosive activity commences; earthquake felt in Chillán. Tephra fall turned water cloudy in the River Ñuble, 20 km north
August 22nd 1861	Lava effusion commences producing the majority of the lava which now remains. Volcano was covered in seasonal snow and ice
October 1861	Lava obstructed upper parts of the Santa Gertrudis Valley, a lake was formed and a lahar flowed down the valley, reaching the River Ñuble and destroying dense forest
February 1862–63	Strombolian explosions continued with eruptions of small lava fountains near the vent. Towards the end of this period activity gradually decreased
November 1864–January 1865	Final few months of activity. No lava was emitted during this time but the eruption plume stretched to Talca Province, 300 km northwest; explosions and earthquakes felt in Concepción, 160 km west; lapilli-sized pyroclasts were deposited on the south-eastern side of the volcano in Termas de Chillán

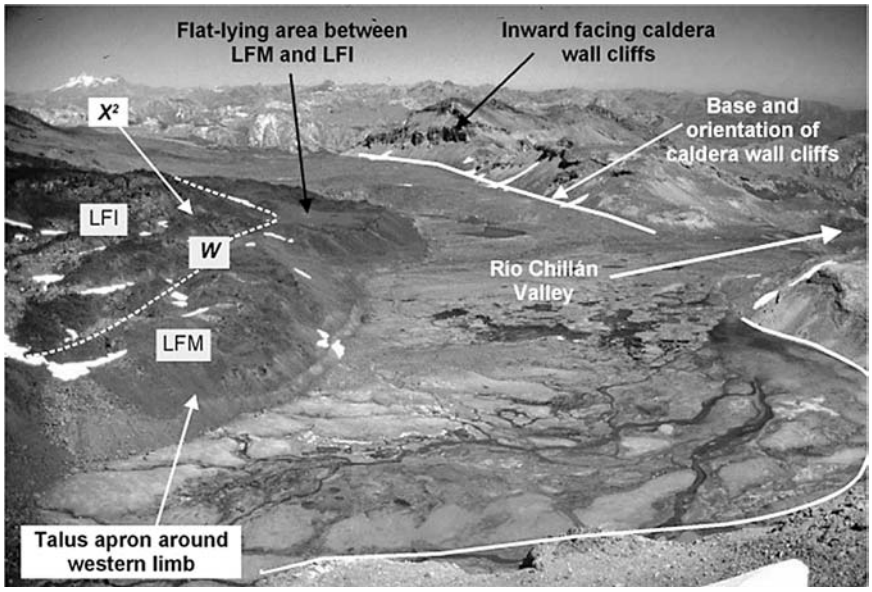

Fig. 4 View looking south towards the arcuate caldera wall cliffs (*solid line*) surrounding the western flank of Cerro Blanco and separated from the western limb (*W*) of the Santa Gertrudis lava (*centre-left*) by a flat-lying area. The *dashed line* marks the boundary between the lava flow margin (*LFM*) and the lava flow interior (*LFI*) and χ^2 refers to the location of Fig. 7. The talus apron is ~5 m high

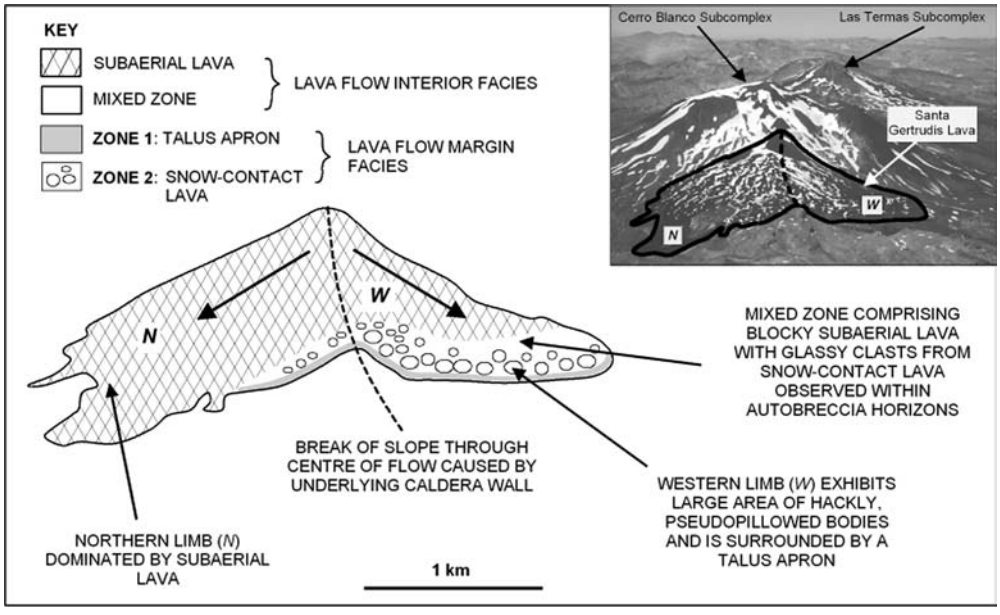

Fig. 5 Schematic diagram of the two limbs of the Santa Gertrudis lava flow showing the distribution of the different facies. Inset shows a photograph of the northwestern flank of Cerro Blanco with the Santa Gertrudis lava flow in the foreground (*highlighted*). Labels *W* and *N* indicate the western and northern flow limbs respectively

in width, where textures are subtly different from the interior facies (Fig. 5). The lava still exhibits blocky, autobrecciated and porphyritic textures similar to the flow interior facies, but also contains clasts unlike that of the flow interior, which are observed within the autobreccia horizons (Fig. 7). The clasts are glassy, vesicle-free and exhibit partial fracture surfaces that may have formed polygons. The angular clasts are glassy and are commonly cut by linear fractures spaced 1–2 cm apart that are perpendicular to the clast surfaces. They contrast with the more crystalline material in the autobreccia although they have an identical phenocryst assemblage. The clasts have the same texture and fracture patterns as the flow margin facies from which they appear to be derived (described in the following section).

There is a 20 m-wide flat-lying area of tephra and scree separating the flow interior from the flow margin on the western limb of the lava (Fig. 4). Although the facies on either side of the flat-lying area exhibit important differences, no contact between the two facies is observed. On the northern limb, once again no contacts are observed between the flow margin, mixed zone and flow interior, but the change in facies type is gradational over several metres and is not concealed by tephra.

Structures seen within the lava flow interior are typical features of subaerially emplaced andesitic lavas (Cas and Wright 1987; McPhie et al. 1993), and hence such a setting is inferred for the majority of the Santa Gertrudis lava. Despite the lava being erupted during the winter (August) of 1861, when the upper slopes of the volcano were covered

in snow and ice (Petit-Breuilh 1995), there is no evidence to suggest that the main body of the flow (i.e. the flow interior facies) came into contact with snow or ice.

Lava flow margin

The margins of the Santa Gertrudis lava, particularly around the western limb where the lava flowed into the flat-lying area inside the caldera wall (Fig. 4), are markedly different in structure and texture to the flow interior. The flow margin can be divided into two zones (Fig. 5): Zone 1 is a glassy talus apron around the outermost sections of the flow, and Zone 2 is a zone of glassy lava lobes.

The outermost zone (Zone 1) of the western limb of the Santa Gertrudis lava is composed of a 5 m-high and 5 m-wide talus apron (Fig. 4). The apron consists of sub-angular clasts of andesite lava, ranging from 10 to 70 cm in diameter and cut by cooling fractures that form columns (or polygons) 1–2 cm in diameter. Zone 1 is glassy throughout and the clasts are identical to those welded onto autobreccia horizons in the mixed zone. The talus apron obscures much of the base of the Santa Gertrudis lava; hence its characteristics are unknown. On the northern limb, Zone 1 is discontinuous and, in places, the Zone 2 lava forms the outermost boundary of the flow (although the base is still obscured by talus and debris).

Zone 2, which appears behind the talus apron, is a 20-m-wide area of dome-shaped lava bodies. They are glassy throughout and slightly elliptical in plan view with their long axes oriented parallel to the flow margin. They can be up to 10 m in length, 1–2 m in height and 2–3 m in width and are extensively fractured.

Complicated fracture patterns are observed throughout the Zone 2 facies and involve intersecting, curved *primary* fractures (Fig. 8). Primary fractures are arcuate, <1 to >5 m in length, with no preferred orientation within individual lava bodies. Primary fractures show varying degrees of curvature, from near-planar to strongly curved, and locally intersect (Fig. 8). The fracture surfaces are glassy and are often coated by coarse-grained glassy ash. A second generation of shorter, *secondary* fractures is also observed. They occur perpendicular to primary fracture surfaces, are spaced 1–5 cm apart and extend up to 10 cm away from the primary fracture. Secondary fractures are polygonal in cross-section, with 3–6 near-planar faces, and are thus similar to columnar joints. The geometry of the intersecting fractures is similar to 'pseudopillow fractures' discussed by Watanabe and Katsui (1976) and Lescinsky and Fink (2000), who describe arcuate fractures extending for several metres with shorter secondary fractures propagating perpendicular to them. The term 'pseudopillow' is used here exclusively to describe fracture geometries and morphology, and not as a genetic interpretation of subaqueously-erupted lava.

Fracture generation

Primary fractures in the Santa Gertrudis lava are thought to have formed when tensile stresses in the lava base, probably due to cooling contraction and melting of supporting snow, exceeded the tensile strength of the lava (e.g. Ryan and Sammis 1978; Lore et al. 2000). Steam is then thought to have penetrated into the fractures at the flow base, and caused rapid chilling of the fracture surfaces. Intersecting of the primary fractures has produced, in some instances, pseudopillow geometries. It is unlikely that the fractures formed simultaneously, because fracture orientations are highly variable and locally cross-cutting. Rotation of fractures by subsequent viscous flow is therefore rejected, since it cannot explain the cross-cutting geometries or the highly variable curvature of fractures.

It is suggested that steam removed heat from the fracture surfaces creating a steep thermal gradient perpendicular to the fracture surfaces and triggering the formation of contractional secondary fractures, which are analogous to columnar joints (e.g. Ryan and Sammis 1978; Aydin and DeGraff 1988; DeGraff and Aydin 1993; Grossenbacher and McDuffie 1995; Lescinsky and Fink 2000; Lore et al. 2000). Because the secondary fractures are always perpendicular to the primary fractures, it is suggested that they were not affected by shear stresses within the lava body and were most likely formed during a later stage of cooling once the stress fields within the lava had become stable. The presence of coarse-grained glassy ash on the surfaces of some primary fractures may be additional evidence for steam fluxing through the fractures, carrying ash formed by magma-meltwater interaction at the lava flow base.

Although a lake is reported to have formed above the Santa Gertrudis Valley along the northern limb of the lava at the time of eruption (Petit-Breuilh 1995), the topography surrounding the western limb is such that any meltwater produced by the eruption would have drained downslope and west into the Chillán River (Fig. 4). So therefore, while an accumulation of meltwater around the northern limb could explain the production of arcuate fractures around the margins in that locality, a similar scenario is unlikely for the western limb. Pseudopillow structures in lava bodies on the western limb are exposed at least 5 m above the level of the drainage outlet to the western valleys. If their formation were due to water penetration, a lake of at least this depth would have had to form, which would have required damming by some means, most likely by the lava itself. However, the lava halted 500 m from the drainage outlet and it is highly unlikely that significant amounts of material have been eroded since 1861. In addition to this, the maximum snow thickness on the western flanks at present day occurs between August and October and is approximately 1.6 m (Gilbert et al. 1998). Assuming winter conditions have not changed significantly since 1861, snow of <5 m thickness would have been insufficient to enable the lava to burrow beneath the snow thus causing meltwater to infiltrate downwards through the structure. The most likely scenario is therefore that lava flowed over snow or small accumulations of meltwater (<1 m depth) and rising steam infiltrated the lava, causing formation of arcuate fractures throughout the entire flow margin. The absence of hyaloclastite exposed throughout the flow margins also supports the theory of cooling by steam rather than wa-

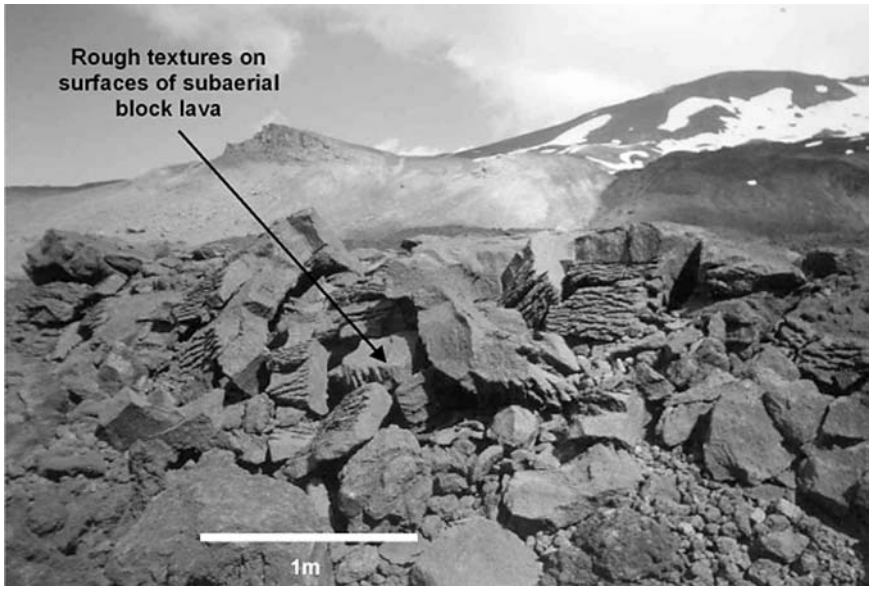

Fig. 6 Subaerial, blocky lava of the interior facies of the Santa Gertrudis lava flow. Located on Fig. 4 as χ^1 and viewed looking SE towards the Cerro Blanco summit

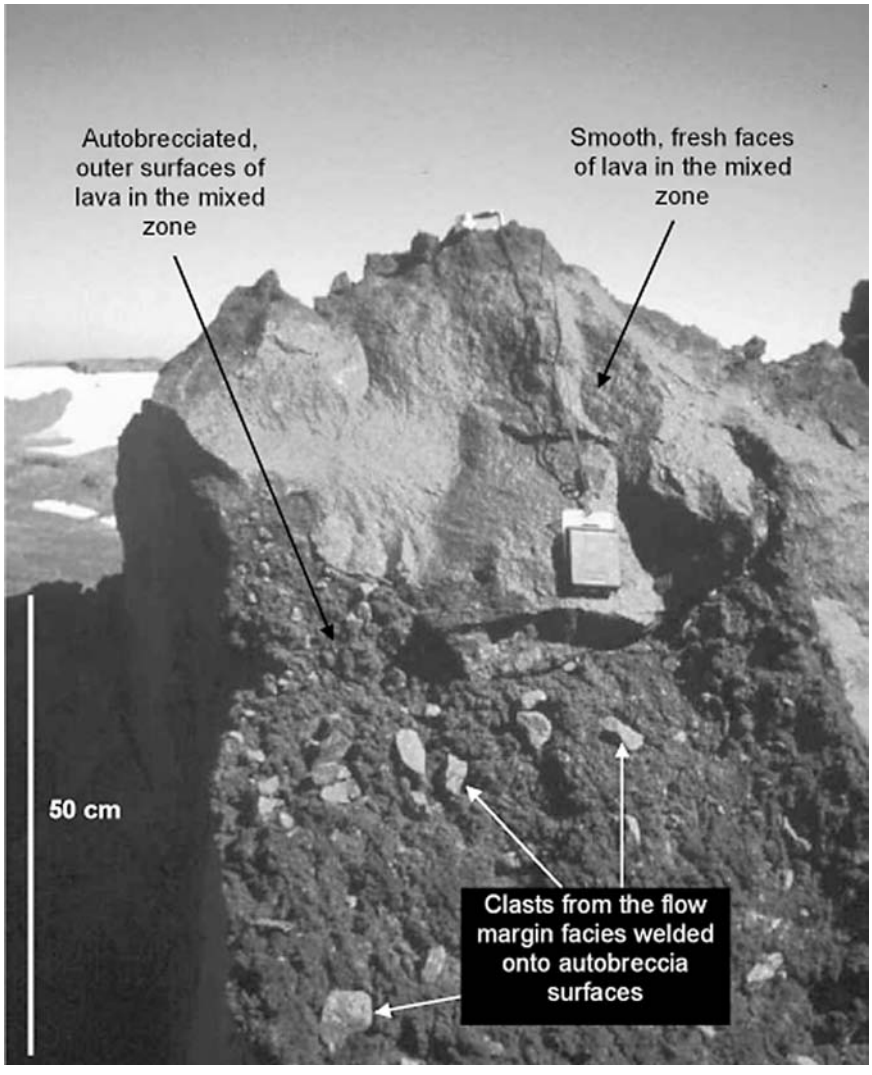

Fig. 7 Mixed zone at the edge of the flow interior facies where clasts thought to have originated from the snow-contact, flow margin facies are welded onto autobreccia horizons of the subaerial lava. Located on Figs. 2 and 4 as χ^2

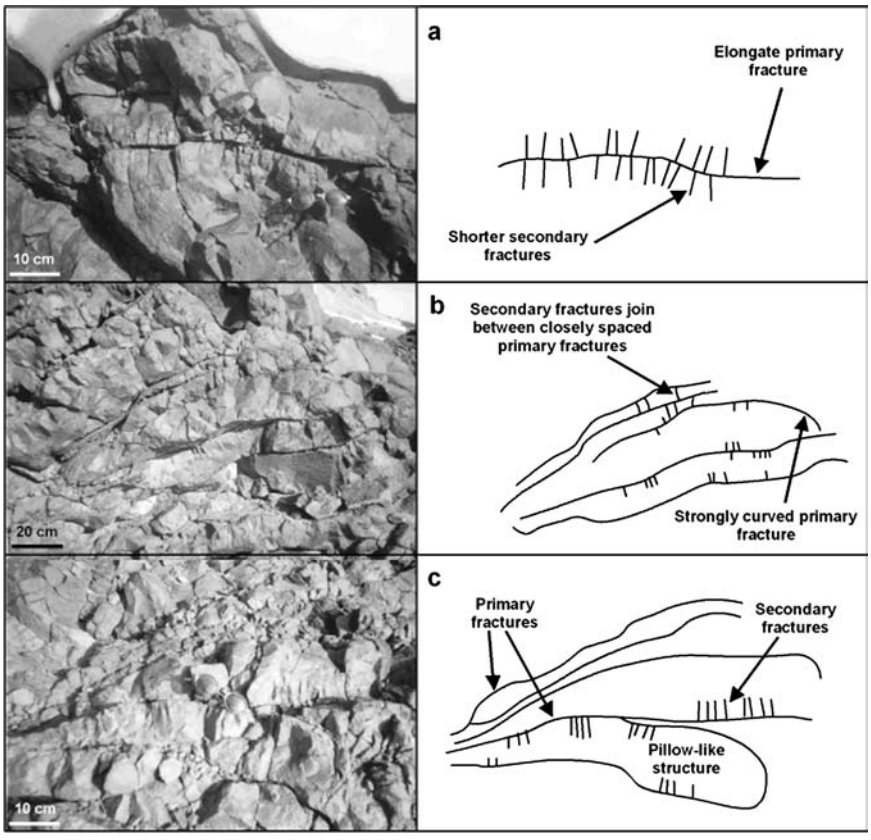

Fig. 8 Typical fracture patterns observed in the flow margin facies of the Santa Gertrudis lava: **a** a long, arcuate primary fracture with shorter secondary fractures propagating perpendicular to it; **b** a set of primary fractures, one of which is strongly curved and intersects a neighbouring primary fracture; **c** a set of primary fractures forming a pillow-like structure

ter in the upper portions of the lava. It is likely that some hyaloclastite was formed at the base of the lava, particularly if small accumulations of meltwater were present, as the current topography suggests; however, because the base of the lava is not exposed, this remains unknown. The talus apron is thought to have formed by gravitational instability of the flow margin facies at the flow front and by continual weathering (e.g. freeze-thaw action).

A similar process of formation is inferred for the arcuate fractures and pseudopillow structures seen on the northern flank. During the 1861 eruption, the lava obstructed the snow-covered upper parts of the Santa Gertrudis Valley, forming a lake, and a lahar was produced in October 1861 (Table 2). The exact location of this lake is unclear, thus it is not possible to determine whether meltwater or steam was responsible for the production of pseudopillow structures on the northern limb. However, their location on the portion of the Santa Gertrudis lava that straddles the caldera wall (i.e. on a topographic high) suggests that a lake would not have formed in that particular location. In addition, the similarities between the fracture types observed on the western and northern limbs and the absence of hyaloclastite suggest that they too were formed by steam infiltration as lava flowed over snow and ice, rather than by water.

Model of emplacement

The variable nature of structures observed within the Santa Gertrudis lava lead us to interpret that the lava was cooled both subaerially and as a result of ice- and snow-contact. The lava shows no evidence of having been confined by a cooling medium and therefore ice-constraint can be ruled out.

It is easily envisaged that the outer margins (and base) of the lava flowed over snow causing extensive fracturing, whilst the flow interior was able to cool subaerially. However, what is less easily explained is how the mixed zone was formed, i.e. how glassy and fractured clasts originating from the flow margins have come to be welded onto autobreccia surfaces of the subaerial flow interior. A model of emplacement (Fig. 9) based on the interpretations discussed above, field observations and eyewitness reports is outlined below.

The first and main period of lava effusion commenced on 22nd August 1861 when the flanks of Cerro Blanco are believed to have been covered in up to 1.6 m thickness of ice and snow, based on current winter estimates (Petit-Breuilh 1995; Gilbert et al. 1998). The initial pulses of lava flowed north towards the Santa Gertrudis Valley and west towards the caldera walls, flowing over snow and ice and causing melting (Fig. 9a). Meltwater accumulated in the Santa Gertrudis Valley, and later generated a lahar. To the west, meltwater drained into the Río Chillán Valley, although small accumulations of <1 m depth may have been present on the flat-lying area to the east of the caldera walls (based on current topography). Steam given off from melting of the underlying snow caused cooling contraction of the lava, which led to the formation of long arcuate primary fractures (Fig. 9b). The fractures then provided a

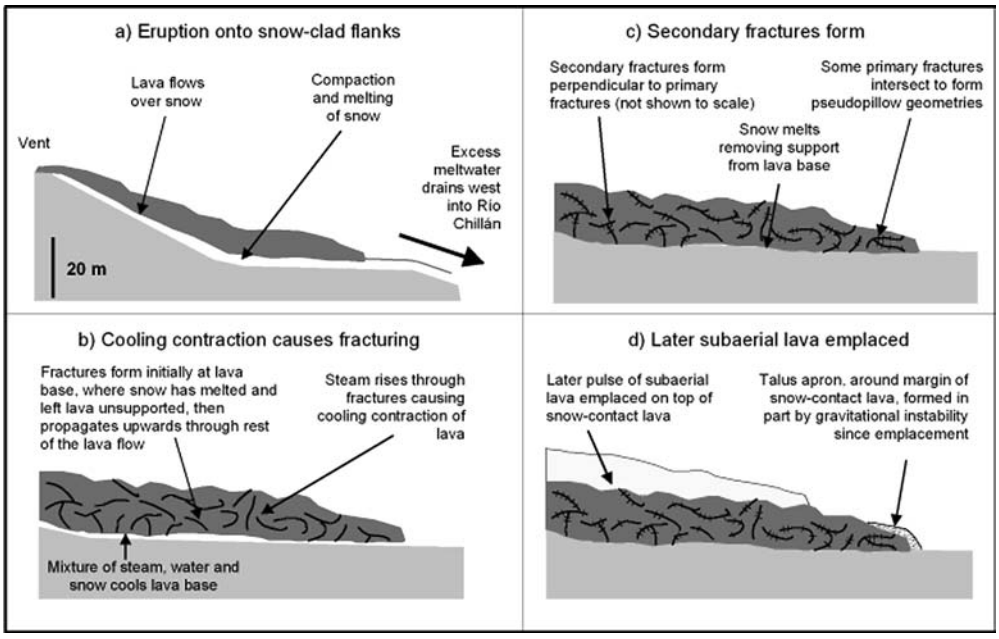

Fig. 9 Schematic model showing suggested emplacement of the Santa Gertrudis lava western limb. See text for full explanation

network of pathways throughout the lava, through which steam could migrate, causing further cooling-contraction and the formation of secondary fractures oriented perpendicular to the primary fractures (Fig. 9c). A later pulse of subaerial lava is hypothesized to have flowed over the earlier snow-contact lava, causing fragments of the glassy pseudopillows to become incorporated onto the autobrecciated base of the subaerial lava (Fig. 9d). As the margins of the upper subaerial lava have collapsed by gravitational instability over the years, portions of the autobrecciated base incorporating glassy pseudopillowed clasts have become exposed. The talus apron around the margin of the lava flow is thought to have been forming continually (since solidification) by gravitational instability of the flow margin facies due to freeze-thaw action after each winter season (during fieldwork seasons, the authors observed regular collapse events along the margins of the lava as summer melting progressed). The Santa Gertrudis lava thus apparently had a two-phase emplacement and cooling history: an early snow-contact phase and a later subaerial phase.

Palaeoenvironment reconstruction in the Upper Santa Gertrudis Valley

Lava flows with similar fracture geometries to the Santa Gertrudis lava occur, in units, elsewhere at Nevados de Chillán and are, through analogy, also interpreted as snow-contact facies. Locally, there are close associations between the snow-contact lava units and those with characteristics of being ice-constrained and cooled by water, which can be used to determine the past distribution and thicknesses of snow and ice on the volcano. Such an exercise can be performed on older lava that is partly overlain by the Santa Gertrudis lava on the northwest flank of the volcano.

The Upper Santa Gertrudis Valley lava

The newly identified Upper Santa Gertrudis Valley (USGV) lava, with an age of 90.0±0.6 ka (Table 1), crops out at 2,300—2,200 m altitude between the northern end of the caldera wall and the top of the Santa Gertrudis Valley (Fig. 10), and is andesitic in composition. It averages ~10–20 m in thickness. Geomorphically, the lava exists in two forms: as isolated or interconnected bulbous bodies at the upper elevations and as a continuous flow unit at the lower elevations. The lava can also be divided on the basis of texture and, in this respect, three zones can be identified based primarily on the geometry and type of fracturing that dominates that particular zone. Sharp contacts between structural or textural zones are not observed and the changes are gradational over several metres. The three zones occur within different elevations between the upper limit at 2,300 m and the lower limit below 2,200 m (Figs. 10 and 11).

Zone 1

Units of the lava assigned to Zone 1 crop out between 2,300 m and 2,260 m altitude (Figs. 10 and 11). Eleven elongate lobes are exposed. The lobes are typically 8–13 m long, 4–6 m wide and 2–3 m high. They usually occur as isolated bodies, although in at least one location two lobes appear to be interconnected. The lava is glassy, contains rounded vesicles up to 4 mm in diameter, and in places has complex flow banding. Fractures similar to those described

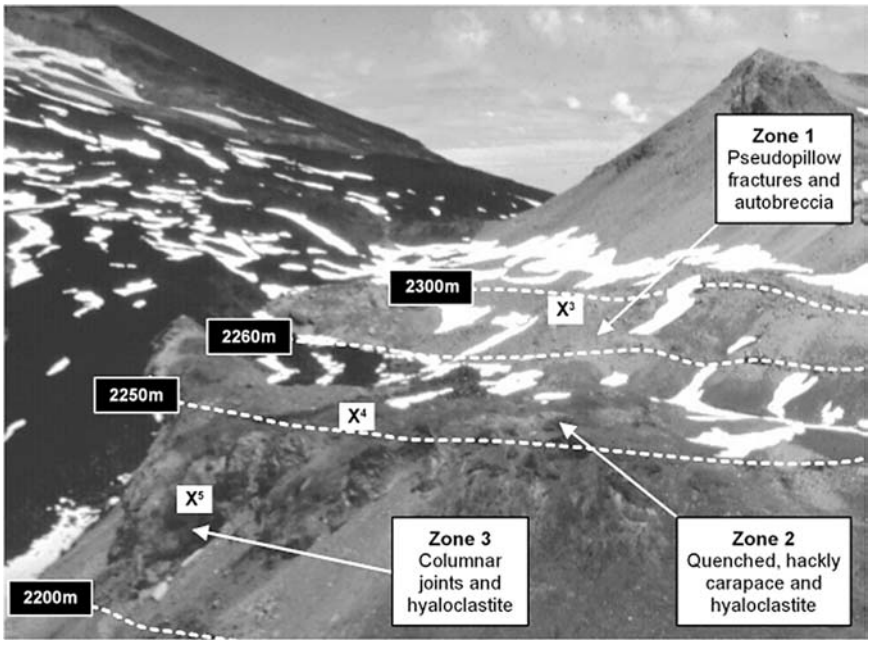

Fig. 10 The Upper Santa Gertrudis Valley (USGV) lava on the northwestern flank of Cerro Blanco, showing the altitudinal limits of the three textural zones. View is from the top of the Santa Gertrudis Valley looking southwest. χ^3, χ^4 and χ^5 refer to the locations of Fig. 12a–c, respectively

in the Santa Gertrudis lava margins can be found in abundance on the Zone 1 lavas (Fig. 12a). These consist of an elongate, often curved primary fracture, usually in excess of 1 m in length. At right angles to the primary fracture is a set of shorter, secondary fractures, which penetrate up to 7 cm into the surrounding rock and are spaced ~1 cm apart. Autobreccia zones are also exposed around the margins of the lobes.

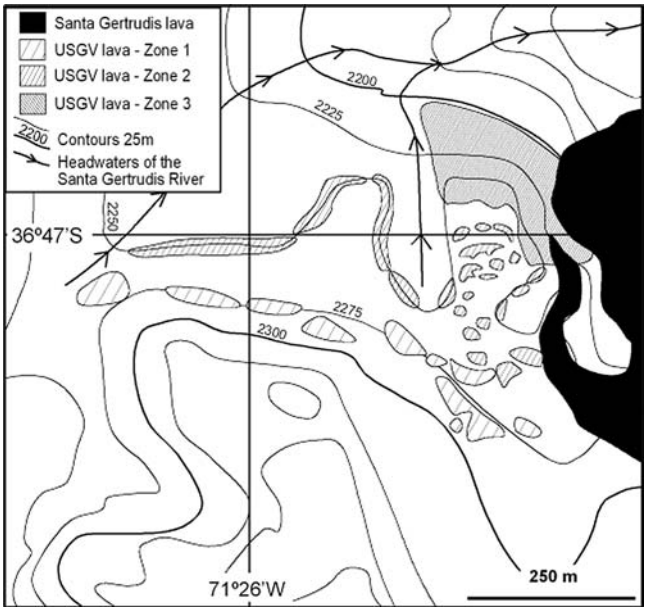

Fig. 11 Map showing the distribution of the three zones of the Upper Santa Gertrudis Valley (USGV) lava and the Santa Gertrudis lava. All other geology between 2,200 and 2,300 m elevation is obscured by talus

Zone 2

Downslope, the land flattens at 2,250-m altitude into a 0.5-km^2 semi-circular plateau which is dominated by a further twenty-four lava lobes (Fig. 11). The majority of these lobes tend to be slightly smaller and more rounded in plan view than those in Zone 1, have typical lengths of 5–10 m and exposed heights of 2–3 m, although some are larger and more elongated. Although several of the lobes appear to be isolated, many are interconnected locally, making it difficult to identify individual lobes. The distinguishing feature of the Zone 2 lobes is the presence of a glassy and hackly jointed outer carapace. Remnants of arcuate fractures can be seen on some lobes but hackly fractures are the dominant fracture type. The hackly fractures intersect to form irregular polygonal blocks (Lescinsky and Fink 2000) on the glassy outer carapace, which penetrate no more than 25 cm into the lobe interior. The centres of the lobes are holocrystalline, similar to the Zone 1 lobes and exhibit platy fractures, which are concordant with the lobe margins. Platy fractures are spaced 1–3 cm apart. In smaller lobes, <1 m in diameter, this platy fracturing is not developed and hackly jointing is observed throughout. Another major difference between the Zone 1 and Zone 2 lobes is the presence of yellow, clast-supported hyaloclastite breccia that surrounds the Zone 2 lobes (Fig. 12b). The contact between the lava lobe and the hyaloclastite is often gradational over ~5 cm. Over a distance of 1 m from the margins of the lava lobes, the clasts in the hyaloclastite grade from ~10 cm in diameter to <5 mm in diameter. The clasts are angular andesite lava and are glassy throughout. The abundance of hyaloclastite breccia over the brink of the plateau edge, where cross-sections through the zone can be seen, is much greater than that on the plateau where it only appears

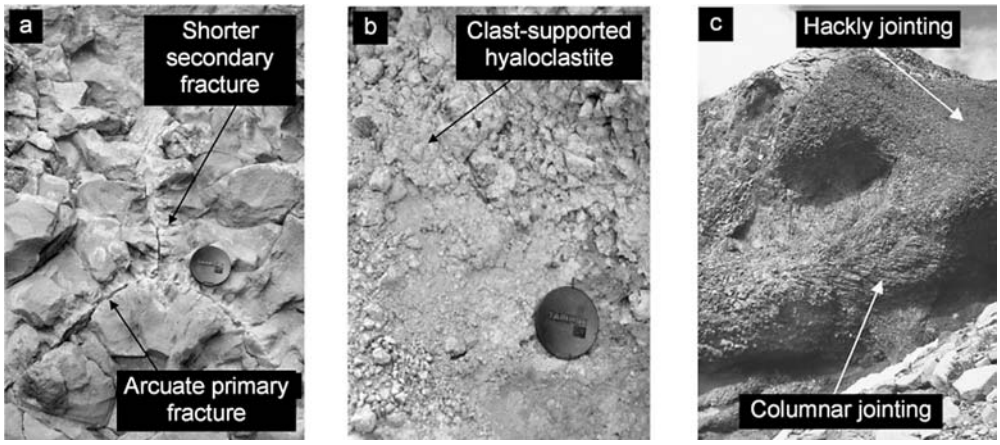

Fig. 12 Structures observed in the various zones of the Upper Santa Gertrudis Valley (USGV) lava: **a** primary and secondary fractures on the Zone 1 lava lobes (χ^3 on Fig. 10); **b** hyaloclastite breccia in Zone 2 (χ^4 on Fig. 10); **c** columnar and hackly joints on the Zone 3 lava (χ^5 on Fig. 10). Lens cap for scale (**a**–**b**) is 8 cm in diameter; field of view is ~10 m across (**c**)

at lobe bases. Beneath the plateau, hyaloclastite breccia can often be seen to surround entire lobes.

Zone 3

Over the edge of the plateau and into the uppermost part of the Santa Gertrudis Valley, the lava takes on a different form and can be followed downslope to below 2,200 m elevation (Figs. 10 and 11). The morphology no longer resembles isolated lobes, but instead is observed as one continuous flow made up of multiple, interconnected lobes that can be traced over several tens of metres down to its lower limit (Fig. 12c). At one locality, the lava forms a 25-m-high lava wall, with a surface slope of 60°. The outer surface of the lava is extremely glassy and exhibits both hackly and columnar jointing (Fig. 12c). The hackly joints tend to appear towards the top of the zone, close to the boundary between Zone 2 and Zone 3, whereas the columnar joints become more dominant further down slope. The columns are narrow, <8 cm wide and penetrate >1 m into the flow. In general, the columns are horizontal to subhorizontal (perpendicular to the slope); although in some localities they appear to be randomly orientated. The interior of the flow is holocrystalline and platy jointed, with the plates forming concentric layers around the flow lobe interiors. Hyaloclastite breccia is also observed at the top of Zone 3 and is predominantly found along the base of the lava. Its apparent thickness is at its greatest (~10 m) in a present-day drainage channel, where it is as thick as the lava that it underlies. On the sloped areas of Zone 3, particularly around the 25-m-high lava wall, hyaloclastite is not preserved.

Although the three lava zones exhibit differing morphologies and textures, their stratigraphic relationships suggest that they were emplaced during a single eruptive episode. The changes in structure occur gradually and the lobes appear, in many places, to be interconnected with no sharp or unconformable contacts observed throughout the entire unit. Compositionally, the mineral assemblages of samples from all three zones are the same, whilst major and trace element abundances are very similar for all samples (Mee 2004, unpublished data). In addition, two identical sets of glacial striae were observed on all zones of the USGV lava, suggesting that each unit has been subjected to the same glaciations. For these reasons, it is suggested that all three zones are part of the same lava field, erupted and emplaced during the same volcanic event.

Interpretation

The arcuate fractures and glassy textures within Zone 1 are thought to have formed in a way analogous to those on the Santa Gertrudis lava: by snow-contact. Steam given off by melting of snow and ice is thought to have caused cooling contraction of the lava followed by the formation of arcuate fractures. 'Ploughing' of the lava into the snow in some localities is thought to have produced the autobreccia on the Zone 1 lobes. A substantial amount of erosion may have occurred since the emplacement of the USGV lava (indicated by the presence of glacial striae and polishing throughout), and any hyaloclastite breccia that existed in Zone 1 may since have been removed. In addition, meltwater is thought to have drained downslope away from the Zone 1 lobes resulting in the relative lack of hyaloclastite in Zone 1 compared to Zones 2 and 3.

In Zone 2, the presence of hyaloclastite is widespread and some cross-sections through the lobes show that hyaloclastite may have entirely surrounded some lobes. It is suggested that a large amount of hyaloclastite has been removed by erosion since its emplacement, supported by the presence of two sets of striae on all zones of the USGV lava, which suggest that they have been affected by at least two major glaciations. Several glaciations have occurred since the eruption of this unit at 90.0±0.6 ka, including the Last Glacial Maximum between 35–18 ka (Clapperton 1993).

The hyaloclastite breccia, and in particular the presence of glassy clasts within the breccia, suggest that water had

an influential role in cooling the Zone 2 lobes. The most feasible source of water in this region is from melting of ice and snow, and since a lake formed in this area during the recent eruption of the Santa Gertrudis lava, it is possible that a similar scenario occurred during the eruption of the USGV lava.

The most striking feature of the Zone 3 lava is the presence of narrow, sub-horizontal columnar joints. Since columnar joints form at right angles to a cooling surface, measurement of their orientations can enable the former cooling surface to be calculated. In this case, the cooling surface was steeply inclined at ~60°. The most likely cooling medium was therefore a steep ice wall (or compacted snow bank) capable of constraining the lava to enable it to solidify at such a steep angle without collapsing (Lescinsky and Sisson 1998; Tuffen et al. 2001). The presence of large amounts of hyaloclastite in places throughout Zone 3 also suggests that water had an influential role. As the thickness of the hyaloclastite is quite irregular along the base of the lava, forming in one area with a thickness similar to that of the overlying lava, it is suggested that water was localised to drainage channels into which the lava flowed. Where the Zone 3 lava is exposed on steep surfaces, it is suggested that any hyaloclastite that formed collapsed under gravity and was washed away downslope.

Palaeoenvironment reconstruction

Global palaeoclimate studies have shown that ice ages and their regional extents are difficult to constrain, hence the absence of a definitive record in the literature. For example, periods of extensive ice in one region might coincide with relatively little ice in another, especially when comparing northern and southern hemispheres, or equatorial regions with higher latitudes. According to global climate studies (e.g. Clapperton 1993), the 90.0±0.6 ka age for the USGV lava suggests that it was emplaced during an interglacial. (Marine Oxygen Isotope Stage 5) similar to today and hence it would generally be assumed that large volumes of ice were not present on Nevados de Chillán. However, global studies have shown that at ca. 90 ka during the MOIS 5 interglacial, climate was cooler than the present day (Fig. 13) (Lowe and Walker 1997), suggesting that snow and ice coverage was actually greater than the current winter average of 1.6 m (Petit-Breuilh 1995; Gilbert et al. 1998), and since snow and ice are present on the volcano all year round (during the current interglacial) it is almost certain that seasonal snow and ice would have existed on Nevados de Chillán at the time of emplacement.

Figure 14 is a schematic reconstruction of the emplacement environment of the USGV lava. We suggest that although the lava was emplaced during an interglacial period, the upper Santa Gertrudis Valley was covered in significant amounts of snow and ice at 90.0±0.6 ka. Zone 1 is thought to have been cooled in a snow-contact environment causing melting of snow and ice at the lava base but without causing confinement of the lava. Arcuate fractures formed by cooling contraction, whilst ploughing of the lava into snow in some localities resulted in the formation of autobreccia. As the lava flowed downslope and onto the plateau, an increasing influence of water caused rapid quenching and solidification of the lobe carapaces, creating the Zone 2 lobes. Penetration of water and steam into cooling lava formed hackly fractures (Lescinsky and Fink 2000). Quench fragmentation generated the hyaloclastite breccia around the lobes (Lescinsky and Fink 2000; Tuffen et al. 2001), much of which appears to have since been

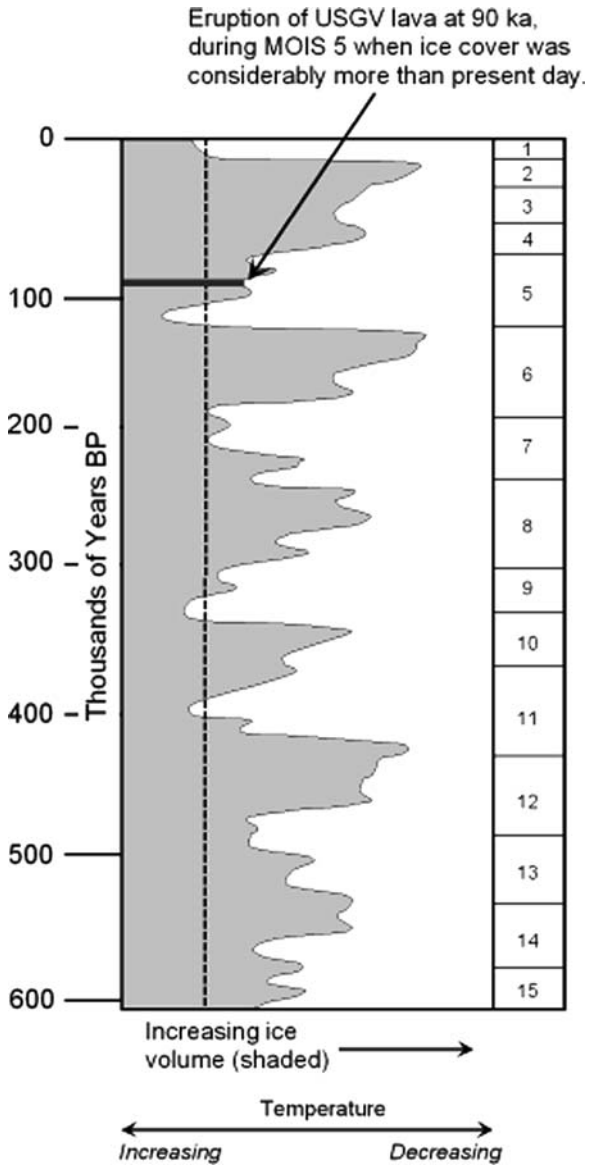

Fig. 13 Schematic representation of oxygen isotope variations for the past 600 ka. Isotopically light values are to the *left* (representing warmer temperatures) and isotopically heavy values are to the *right* (representing colder temperatures). The *dashed vertical line* represents the isotope ratio that corresponds to the limited ice cover typical of the late Holocene. Notice how the temperature at 90 ka when the USGV lava was erupted is lower than that of present day making it very likely that ice cover was considerably more than today (modified after Broecker and Denton 1990)

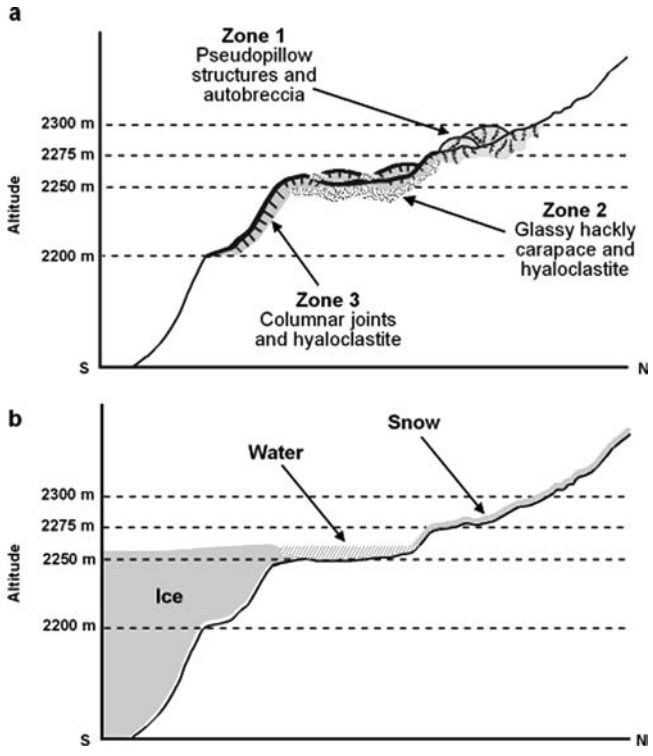

Fig. 14 Schematic model of the emplacement environment of the Upper Santa Gertrudis Valley (USGV) lava: **a** distribution of fracture types associated with each zone of the USGV lava; **b** the suggested environment into which each zone was emplaced. Not to scale

removed by erosion. The abundance of hyaloclastite breccia is consistent with the presence of ponded water at that elevation during eruption. Melting of snow from the initial snow-contact in Zone 1 may have caused increased volumes of meltwater to form a lake on the plateau and it is suggested that the lava flowed into a lake or a network of meltwater channels on the plateau, producing the fracture types seen in Zone 2. Finally it is suggested that lava reached and flowed over the plateau edge into the upper Santa Gertrudis Valley, which we suggest contained a small valley glacier against which the USGV lava abutted and cooled resulting in ice-constrained textures in Zone 3. Evidence for this comes from the presence of gently dipping columnar joints, which indicate a cooling surface dipping at ~60°, a feature considered typical of ice-constrained lavas (Lescinsky and Sisson 1998; Tuffen et al. 2001, 2002a).

The implication is that the more exposed, higher altitude areas that Zone 1 and Zone 2 were emplaced into were covered by snow, whereas the more sheltered Upper Santa Gertrudis Valley was filled with a small valley glacier. Since the Santa Gertrudis lava overlies much of this region it is not possible to determine how extensive this glacier or the USGV lava may have been. However, the transition from non-constraining snow and ice to glacial ice can be determined by measuring the altitude at which snow-contact features become ice-constrained features (Fig. 14). This occurs at 2,250 m on the USGV lava, which we believe marks the approximate upper limit of the valley glacier during the time of emplacement (Fig. 14).

Conclusions

1. Identification of volcanic facies characteristic of subaerial, subglacial, ice-constrained and snow and/or ice-contact activity is important for establishing past eruptive environments and particularly for establishing palaeoenvironmental conditions at the time of an eruption.
2. Pseudopillow fractures formed in lava emplaced in a nineteenth century eruption are interpreted as snow- or ice-contact features, and differ distinctly from ice-constrained and subaerial lava facies.
3. Similar textures in lava dated at 90 ka BP are used to reconstruct the distribution of snow and ice on the stratovolcano during the MOIS 5 interglacial.
4. Global climate studies have shown that at ca. 90 ka, temperatures were cooler than at present day and hence it is likely that greater thicknesses of ice and snow were present at the time of eruption and support the presence of a small valley glacier in the Santa Gertrudis Valley.
5. The use of snow- and/or ice-contact and ice-constrained lavas may be applied to reconstruct changing ice thicknesses and extents of snow cover in the Chilean Andes and elsewhere.

Acknowledgements This project was supported by a NERC Studentship. We wish to thank J. Naranjo of the Servicio Nacional de Geología y Minería, Chile, for his valuable insight in the field and continual suggestions to the project. Many thanks to Malcolm Pringle for $^{40}Ar/^{39}Ar$ analysis at the Scottish Universities Research Reactor Centre (SURRC), East Kilbride. Thanks to Mike James, Dave McGarvie, Andy Lee and Maialen Galarraga for field assistance and to David Lescinsky, John Smellie and Ian Skilling whose valuable reviews have substantially improved this paper. Finally, many thanks to Lionel Wilson and Dave McGarvie, whose detailed suggestions have been gratefully accepted.

References

Aydin A, DeGraff JM (1988) Evolution of polygonal fracture patterns in lava flows. Science 239:471–476

Barberi F, Coltelli M, Frullani A, Rosi M, Almeida E (1995) Chronology and dispersal characteristics of recently (last 5000 years) erupted tephra of Cotopaxi (Ecuador): implications for long-term eruptive forecasting. J Volcanol Geotherm Res 69(3/4):217–239

Broecker WS, Denton GH (1990) What drives glacial cycles? Sci Am 262:42–50

Cas RAF, Wright JV (1987) Volcanic successions: modern and ancient. Chapman, London pp. 528

Clapperton CM (1993) Quaternary geology and geomorphology of South America. Elsevier, Amsterdam, pp 779

DeGraff JM, Aydin A (1993) Effect of thermal regime on growth increment and spacing of contraction joints in basaltic lava. J Geophys Res 98(B4):6411–6430

Déreulle B, Déreulle J (1974) Los volcanes Cuaternarios de los Nevados de Chillán y reseña sobre el volcanismo Cuaternario de los Andes Chilenos. Estud Geol 30:91–108

Dixon HJ, Murphy MD, Sparks RSJ, Chávez R, Naranjo JA, Dunkley PN, Young SR, Gilbert JS, Pringle MR (1999) The geology of Nevados de Chillán volcano, Chile. Revista Geológica de Chile 26(2):227–253

Edwards BR, Russell JK, Anderson RG (2002) Subglacial, phonolitic volcanism at Hoodoo Mountain volcano, northern Canadian Cordillera. Bull Volcanol 64(3/4):254–272

Gardner CA, Neal CA, Waitt RB, Janda RJ (1994) Proximal pyroclastic deposits from the 1989–1990 eruption of Redoubt volcano, Alaska: stratigraphy, distribution and physical characteristics. J Volcanol Geotherm Res 62(1–4):213–250

Gilbert JS, Sparks RSJ, Young SR (1998) Volcanic hazards at Volcán Nevados de Chillán, Chile. British Geological Survey Technical Report WC/98/14, British Geological Survey, Nottingham, UK

Grossenbacher KA, McDuffie SM (1995) Conductive cooling of lava: columnar joint diameter and striae width as a function of cooling rate and thermal gradient. J Volcanol Geotherm Res 69:95–103

Gudmundsson MT, Sigmundsson F, Björnsson H (1997) Ice-volcano interaction of the 1996 Gjálp subglacial eruption, Vatnajökull, Iceland. Nature 389:954–957

Helgason J, Duncan RA (2001) Glacial-interglacial history of the Skaftafell region, southeast Iceland, 0–5 Ma. Geology 29(2):179–182

Jones JG (1970) Intraglacial volcanoes of the Laugarvatn region, southwest Iceland, II. J Geol 78:127–140

Lescinsky DT, Fink JH (2000) Lava and ice interaction at stratovolcanoes: Use of characteristic features to determine past glacial extents and future volcanic hazards. J Geophys Res 105(B10):23,711–23,726

Lescinsky DT, Sisson TW (1998) Ridge-forming, ice-bounded lava flows at Mount Rainier, Washington. Geol 26(4)351–354

Lowe JJ, Walker MJC (1997) Reconstructing Quaternary Environments (2nd edn), Prentice-Hall, Englewood Cliffs, NJ, pp 446

Lore J, Gao H, Aydin A (2000) Viscoelastic thermal stress in cooling basalt flows. J Geophys Res 105(B10):23695–23710

Major JJ, Newhall CG (1989) Snow and ice perturbation during historical volcanic eruptions and the formation of lahars and floods. Bull Volcanol 52:1–27

Mathews WH (1951) The Table, a flat-topped volcano in southern British Columbia. Am J Sci 249:830–841

McPhie J, Doyle M, Allen R (1993) Volcanic textures; a guide to the interpretation of textures in volcanic rocks. Tasmanian Government Printing Office, Tasmania, pp 196

Mee K (2004) The use of volcanic facies as tools for reconstructing former eruptive environments at Nevados de Chillán volcano, Chile. Lancaster University, Lancaster, UK

Moore JG, Calk LC (1991) Degassing and differentiation in subglacial volcanoes, Iceland. J Volcanol Geotherm Res 46:157–180

Moore JG, Hickson CJ, Calk LC (1995) Tholeiitic-alkalic transition at subglacial volcanoes, Tuya region, British Columbia, Canada. J Geophys Res 100:24577–24592

Petit-Breuilh M-E (1995) The volcanic history of Nevados de Chillán volcano, Chile. British Geological Survey Technical Report WC/95/86, Nottingham, UK

Ryan MP, Sammis CG (1978) Cyclic fracture mechanisms in cooling basalt. Geol Soc Am Bull 89:1295–1308

Skilling IP (1994) Evolution of an englacial volcano: Brown Bluff, Antarctica. Bull Volcanol 56:573–591

Smellie JL (2000) Subglacial eruptions. In: Sigurdsson H (ed) Encyclopedia of Volcanoes Academic, San Diego, California, 403–418

Smellie JL (2001) Lithostratigraphy and volcanic evolution of Deception Island, South Shetland Islands. Antarct Sci 13:188–209

Smellie JL (2002) The 1969 subglacial eruption on Deception Island (Antarctica): events and processes during an eruption beneath a thin glacier and implications for volcanic hazards. In: Smellie JL, Chapman MG (eds) Volcano-ice interaction on Earth and Mars. Geol Soc London Spec Publ 202:59–80

Smellie JL, Skilling IP (1994) Products of subglacial volcanic eruptions under different ice thicknesses: two examples from Antarctica. Sediment Geol 91:115–129

Thouret JC, Cantagrel J-M, Robin C, Murcia A, Salinas R, Cepeda H (1995) Quaternary eruptive history and hazard-zone model at Nevado del Tolima and Cerro Machin volcanoes, Colombia. J Volcanol Geotherm Res 66(1–4):397–426

Tuffen H, Gilbert JS, McGarvie DW (2001) Products of an effusive subglacial eruption: Bláhnúkur, Torfajökull, Iceland. Bull Volcanol 63:179–190

Tuffen H, McGarvie DW, Gilbert JS, Pinkerton H (2002a) Physical volcanology of a subglacial-to-emergent rhyolitic tuya at Rauufossafjöll, Torfajökull, Iceland. In: Smellie JL, Chapman MG (eds) Volcano-ice interaction on Earth and Mars. Geol Soc London Spec Public 202:213–236

Tuffen H, Pinkerton H, McGarvie DW, Gilbert JS (2002b) Melting of a glacier base during a small-volume subglacial rhyolite eruption: evidence from Bláhnúkur, Iceland. Sediment Geol 149:183–198

Vinogradov VN, Murav'ev YD (1988) Lava-ice interaction during the 1983 Klyuchevskoi eruption. Volcanol Seismol 7:39–61

Walder JS (2000) Pyroclast/snow interactions and thermally driven slurry formation. I. Theory for monodisperse grain beds. Bull Volcanol 62:105–118

Watanabe K, Katsui Y (1976) Pseudo-pillow lavas in the Aso caldera, Kyushu, Japan. J Mineral Petrol Econ Geol 71:44–49

Werner R, Schmincke HU, Sigvaldason G (1996) A new model for the evolution of table mountains: volcanological and petrological evidence from Herdubreid and Herdubreidartogl volcanoes (Iceland). Geol Rundschau 85:390–397

Wilch TI, McIntosh WC (2000) Eocene and Oligocene volcanism at Mount Petras, Marie Byrd Land: implications for middle Cenozoic ice sheet reconstructions in West Antarctica. Antarct Sci 12(4):477–491